

3. Basin, V. K. & Trager, W. 1984. Gametocyte-forming and non-gametocyte-forming clones of *Plasmodium falciparum*. *Am. J. Trop. Med. Hyg.*, **33**:534-537.
4. Carter, R. & Miller, L. H. 1979. Evidence for environmental modulation of gametocytogenesis in *Plasmodium falciparum* in continuous culture. *Bull. WHO*, **57**(Suppl. 1):37-52.
5. Clark, M. R. 1988. Senescence of red blood cells: progress and problems. *Physiol. Rev.*, **68**:503-554.
6. Downs, W. G. 1947. Infection of chicks with single parasites of *Plasmodium gallinaceum* Brumpt. *Am. J. Trop. Med.*, **46**:41-44.
7. Fabry, M. E., Mears, J. G., Patel, P., Schaefer-Rego, K., Carmichael, K., Martinez, G. & Nagel, R. L. 1984. Dense cells in sickle cell anemia: the effects of gene interaction. *Blood*, **64**:1042-1046.
8. Friedman, M. J. 1978. Erythrocytic mechanism of sickle cell resistance to malaria. *Proc. Natl. Acad. Sci. USA*, **75**:1994-1997.
9. Garnham, P. C. C. 1966. *Malaria Parasites*. Blackwell Scientific Publications, Oxford, 1114 pp.
10. Jensen, J. B. & Trager, W. 1977. *Plasmodium falciparum* in culture: use of outdated erythrocytes and description of the candlejar method. *J. Parasitol.*, **63**:883-886.
11. Luzzato, L. 1979. Genetics of red cells and susceptibility to malaria. *Blood*, **54**:961-976.
12. Ono, T. & Nakabayashi, T. 1990. Gametocytogenesis induction by ammonium compounds in cultured *Plasmodium falciparum*. *Int. J. Parasitol.*, **20**:615-618.
13. Pasvol, G., Wilson, R. J. M., Smalley, M. E. & Brown, J. 1978. Separation of viable schizont-infected red cells of *Plasmodium falciparum* from human blood. *Ann. Trop. Med. Parasitol.*, **72**:87-88.
14. Ramachandran, L. & Abraham, E. C. 1989. Age-dependent variation in the cytosol/membrane distribution of red cell protein kinase-C. *Am. J. Hematol.*, **31**:69-70.
15. Read, L. K. & Mikkelsen, R. B. 1991. Comparison of adenylate cyclase and cAMP-dependent protein kinase in gametocytogenic and nongametocytogenic clones of *Plasmodium falciparum*. *J. Parasitol.*, **77**:346-352.
16. Reese, R. T., Langreth, S. G. & Trager, W. 1979. Isolation of stages of the human parasite *Plasmodium falciparum* from culture and from animal blood. *Bull. WHO*, **57**(Suppl. 1):53-61.
17. Schneweis, S., Maier, W. A. & Seitz, H. W. 1991. Haemolysis of infected erythrocytes—a trigger for formation of *Plasmodium falciparum* gametocytes? *Parasitol. Res.*, **77**:458-460.
18. Trager, W. 1979. *Plasmodium falciparum* in culture: improved continuous flow method. *J. Protozool.*, **26**:125-129.
19. Trager, W. & Gill, G. S. 1989. *Plasmodium falciparum* gametocyte formation in vitro: its stimulation by phorbol diesters and by 8-bromo cyclic adenosine monophosphate. *J. Protozool.*, **36**:451-454.
20. Walliker, D. 1989. Genetic recombination in malaria parasites. *Exp. Parasitol.*, **69**:303-309.

Received 1-17-92; accepted 1-24-92

J. Protozool., 39(3), 1992, pp. 432-440
© 1992 by the Society of Protozoologists

The Light and Electron Microscopic Cytology of *Janacekia adipophila* N. Sp. (Microspora, Tuzetiidae), a Microsporidian Parasite of *Ptychoptera paludosa* (Diptera, Ptychopteridae)

J. I. RONNY LARSSON

Department of Zoology, University of Lund, S-223 62 Lund, Sweden

ABSTRACT. The microsporidium *Janacekia adipophila* n. sp., a parasite of *Ptychoptera paludosa* larvae in Sweden, is described based on light microscopic and ultrastructural characteristics. Merogonial stages and sporonts are diplokaryotic. Merozoites are formed by rosette-like division. Sporonts develop into sporogonial plasmodia with isolated nuclei. These plasmodia give rise to 8-16 sporoblasts by rosette-like budding. A sporophorous vesicle is initiated by the sporogonial plasmodium. Sporoblasts and spores are enclosed in individual sporophorous vesicles. Granular inclusions of the vesicles, visible using light microscopy, discriminate sporogonial stages from stages of the merogony. The monokaryotic, fresh spores are oval with blunt ends, measuring 4.2-6.3 × 9.1-11.2 µm. Macrospores are formed in small numbers. The spore wall has three subdivisions and the exospore is electron-dense. The polaroplast has two parts: closely arranged lamellae anteriorly, wider sac-like compartments posteriorly. The isofilar polar filament, 191-264 nm wide, has 12-13 coils, which are arranged in one layer in the posterior half of the spore. The electron-dense inclusions of the sporophorous vesicle are modified during sporogony, and vesicles with mature spores are traversed by 21-27 nm wide tubules, which connect the exospore with the envelope of the vesicle. The walls of the tubules, the envelope of the vesicles, and the surface layer of the exospore are all identical double-layered structures. The microsporidium is compared to microsporidia of Ptychopteridae and Tipulidae and to related microsporidia of the family Tuzetiidae.

Key words. Morphogenesis, sporophorous vesicle, taxonomy.

THE family Tuzetiidae was established for microsporidia with a unique type of sporogony: the sporophorous vesicle divides together with the sporogonial plasmodium producing sporoblasts enclosed in individual sporophorous vesicles [12]. The characteristics of the family are shared by microsporidia with isolated nuclei in all life cycle stages and by microsporidia with diplokarya in the early part of their development. Until 1984, *Tuzetia* Maurand, Fize, Fenwick and Michel, 1971 was the only genus of the family. As the type species, *Tuzetia infirma* (Kudo, 1921), lacks diplokarya, *Janacekia* and one more genus were established to accommodate *Tuzetia*-like microsporidia with diplokarya in the early part of their life cycle [6]. *Janacekia* contains two species, which are parasites of blackfly larvae (family Simuliidae).

A microsporidium of the *Janacekia*-type is a locally common parasite of *Ptychoptera* larvae in southern Sweden. *Ptychoptera* are crane fly-like insects, living in fresh water habitats rich in decaying plant material. The microsporidium, which is new to science, is briefly described herein with emphasis on the ultrastructural cytology.

MATERIALS AND METHODS

Microsporidia were obtained from two populations of *Ptychoptera* larvae in the province of Scania, in southern Sweden. Samples were collected in the small river Vege å, at Knutstorp, in the summers of 1987 and 1988, and in a small stream about 500 m from its affluence into the river Rönne å, at Djupadalsmölla, in the autumns of 1989 and 1990. The genus *Ptychoptera*

comprises eight Scandinavian species [13]. As no identification key to the species level exists for the Scandinavian species, the larvae were identified using a British key [2]; however, the British key does not cover all the Scandinavian species. The larvae were identified as *Ptychoptera paludosa* Meigen, 1804, a species previously known to occur in the area.

Fresh squash preparations were made by the agar method of Hostounský and Žižka (Hostounský, Z. & Žižka, Z. 1979. A modification of the "agar cushion method" for observation and recording microsporidian spores. *J. Protozool.*, 26:41A–42A) and studied using phase contrast microscopy and dark field illumination.

Permanent squash preparations were lightly air-dried and fixed in Bouin-Dobuscq-Brasil solution for at least one hour. For paraffin sectioning, parts of larvae or whole larvae were fixed in the same solution or in 4% formalin overnight or longer. After washing and dehydration in a graded series of ethanol, specimens were cleared in butanol and embedded in Paraplast (Lancer, St. Louis, MO, USA). Sections were cut longitudinally at 10 µm. Squash preparations and sections were stained using Giemsa solution or Heidenhain's haematoxylin. For details on the histological techniques used see the manual by Romeis [11]. All permanent preparations were mounted in D.P.X. (BDH Chemicals Ltd., Poole, England). Measurements were made with an eyepiece micrometer at $\times 1,000$.

For transmission electron microscopy, small pieces of infected fat body lobes were excised and fixed in 2.5% (v/v) glutaraldehyde in 0.2 M sodium cacodylate buffer (pH 7.2) at 4° C for 24, 26 or 89 h. After washing in cacodylate buffer and post fixing in 2% (w/v) osmium tetroxide in cacodylate buffer for 1 h at 4° C, tissues were washed and dehydrated in an ascending series of buffer-acetone solutions to absolute acetone and embedded in epon. Sections were stained using uranyl acetate and lead citrate [10].

For scanning electron microscopy, spores were smeared on circular cover glasses, lightly air-dried, and fixed in 2.5% glutaraldehyde in cacodylate buffer at 4° C for 26 h. After washing in buffer and critical point drying, smears were covered with gold and palladium.

RESULTS

Prevalence and pathology. *Ptychoptera* larvae were never found in great quantities. The richest sample, collected on October 4, 1989, contained 13 specimens, 10 of which were infected. Healthy larvae are transparent and have fat body lobes visible as shining white strands. In mixed samples the more chalky white tone and the swollen appearance of the fat body lobes revealed the infected specimens. All specimens were checked for infection microscopically.

Only the adipose tissue harboured microsporidia. Areas with microsporidia-filled cells alternated with healthy ones in all parts of the body (Fig. 1). Nuclei of host cells were hypertrophic. Infected cells were successively destroyed and the lobes turned into syncytia where nuclei and organelles of the host cell were mixed with microsporidia (Fig. 1, 2).

Presporal stages and life cycle. The merogonic part of development was nearly finished in all specimens studied. The last sequence of merogony was revealed by rosette-like dividing plasmodia with diplokaryotically arranged nuclei (Fig. 3) and by groups of more or less rounded diplokaryotic cells (Fig. 4). It is unknown if there is more than one series of merogonic divisions. The number of merozoites per meront is probably variable. Dividing plasmodia with up to five lobes and groups with up to 10 aggregated merozoites were seen. The largest

stained merozoites were 13.4 µm wide, and the largest diameter across a diplokaryon measured 9.8 µm.

Merozoites had a plasma membrane approximately 8 nm thick and a granular cytoplasm with numerous free ribosomes (Fig. 5). There were only traces of rough endoplasmic reticulum. Nuclei had an envelope consisting of two unit membranes, a perinuclear cisterna, and pores.

The last generation of merozoites matured to sporonts. Their volume increased and the two components of the diplokaryon moved apart (Fig. 4). Stained binucleate sporonts measured up to 19.6 µm in diameter, stained nuclei up to 14.2 µm. Centriolar plaques were visible before the nuclei of the diplokaryon separated, at a time when the cells could not be classified as sporonts from cytological evidence (Fig. 5). Plaques appeared as electron-dense areas in shallow depressions of the nuclear envelope. Sectioned plaques were up to 248 nm wide. The first nuclear division of the sporont was probably meiotic, but neither synaptonemal complexes nor other signs of reductional division were observed.

Sporogony proceeded by the production of plasmodia with isolated nuclei (Fig. 6, 7). Uninucleate sporoblasts were released from these plasmodia by rosette-like budding (Fig. 8, 9). Dividing plasmodia had 8–16 lobes, which indicated a yield of 8–16 sporoblasts per sporont. Living sporoblasts were spherical (Fig. 15), and the more or less rounded shape was retained in fixed and stained preparations (Fig. 14). Stained sporoblasts measured up to 10 µm in diameter, and the nucleus was up to 4.5 µm wide. The cytoplasm of sporogonial plasmodia was uniformly granular with numerous ribosomes (Fig. 10). The rough endoplasmic reticulum, with only a few cisternae, was more weakly developed than in sporogonial stages of other microsporidia (Fig. 11). Centriolar plaques and the intranuclear, approximately 20 nm wide, mitotic spindle tubules were identical at the onset of sporogony and in sporogonial plasmodia.

Using light microscopy, undivided and dividing sporogonial plasmodia and sporoblasts were easily discriminated from merogonial stages by having a prominent granulation, visible both in living and stained specimens (Fig. 6–9, 14–15). The granules, measuring 1–2 µm, were inclusions of the sporophorous vesicle, the latter being formed after the first nuclear divisions occurred. Electron-dense material, released from the plasma membrane, formed protuberances, delimiting episporontal spaces more or less filled with electron-dense material (Fig. 10). Continuous production of vesicle material resulted in protuberances increasing in size; and, in addition, the same electron-dense substance covered the cell surface between the vesicle primordia. Sporoblasts had complete individual sporophorous vesicles at the time they were released, but protuberances were still prominent (Fig. 11–13). Inside the envelope of the vesicle the primordia of the exospore appeared as narrow strands of electron-dense material external to the plasma membrane, and these strands increased to completely cover the membrane with a layer of closely and regularly arranged, approximately 22 nm wide, electron-dense, cylindrical fibrils (Fig. 13). The uniformly electron-dense inclusions of the episporontal space degraded to form spongy structures in sporogonial plasmodia (Fig. 11), and paracrystalline arrays of approximately 43 nm wide, globular structures in sporoblasts (Fig. 13). The components of the paracrystalline configurations were globular in all sections; it is therefore more probable that we are dealing with spherical components than with closely arranged fibrils. The material of the inclusions converged to form tubules, approximately 20 nm in diameter, traversing the episporontal space (Fig. 22). Until this time the envelope of the vesicle was about 7 nm thick and uniformly electron-dense. The sporoblasts matured to spores, and the spor-

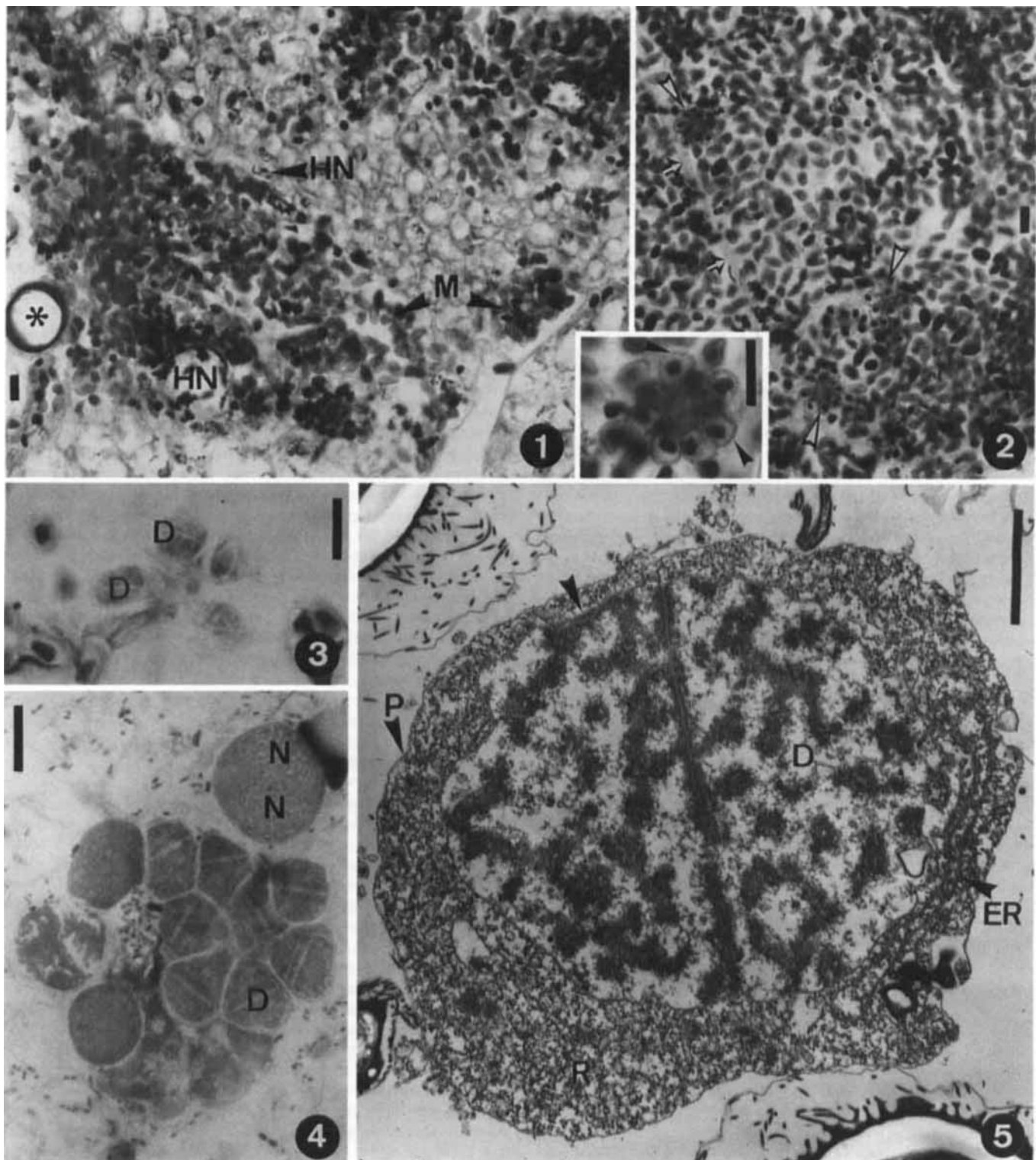


Fig. 1-5. Pathology and merogonic development of *Janacekia adipophila* n. sp. 1. Sectioned fat body lobes of a *Ptychoptera* larva where microsporidia-filled areas alternate with healthy ones. * indicates a transversely sectioned tracheal tube. 2. Detail of a fat body lobe filled with microsporidia. Arrows, the basal membrane of the lobes; arrowheads, rosette-like budding plasmodia. Inset: sectioned rosette-like plasmodium at greater magnification. 3. Rosette-like dividing merogonial plasmodium with five lobes. 4. A group of diplokaryotic merozoites and one merozoite transforming into a sporont. The two nuclei of the diplokaryon are beginning to separate. 5. Ultrathin sectioned cell intermediate to merozoite and sporont. The thick sporont wall has not been initiated yet, but the presence of centriolar plaques (arrowhead) indicates that the nuclei are preparing for division. D, diplokaryon; ER, endoplasmic reticulum; HN, host nucleus; M, microsporidia; N, nucleus; P, plasma membrane. Stains: 1, 2, haematoxylin; 3, 4, Giemsa. Bars: 1-4, 10 μ m; 5, 1 μ m.

al organelles were initiated and developed in the usual way: the polar filament originating from a Golgi apparatus close to the nucleus in the posterior half of the immature spore and the polaroplast being formed around the polar filament at the time it approached the anterior pole of the spore.

Spores. Mature spores were oval with blunt ends (Fig. 15, 16). The posterior end was somewhat broader. Unfixed spores measured $4.2-6.3 \times 9.1-11.2 \mu\text{m}$, fixed and stained spores $3.8-5.6 \times 7.1-9.6 \mu\text{m}$. Macrospores, measuring up to $6.7 \times 16.5 \mu\text{m}$ (fixed and stained), were produced in small numbers (Fig. 17). When stained with haematoxylin or Giemsa, the center of the spores was darker than the poles, which is normal for microsporidian spores (Fig. 16). Haematoxylin revealed the straight part of the polar filament (Fig. 16).

The spore wall was 106–490 nm thick. It had the normal three components: an internal approximately 8 nm thick plasma membrane, a median electron-lucent endospore, and an electron-dense exospore (Fig. 22, 24, 25). The size of the endospore varied from 55 nm, at the anterior pole, to a maximum of 349 nm. The exospore was ornamented with a system of ridges (Fig. 22, 25). Longitudinally and transversely sectioned spores had identical exospores, which indicated that the ridges were winding over the surface or forming a reticulum, not arranged into lines in regular order. The exospore was equally thick all over the spore. At the bottom of the ridges the thickness was about 34 nm. The maximum height of the ridges was 170 nm. The exospore had a uniformly electron-dense basal structure and a 5–7 nm thick two-layered surface component (Fig. 24). The double-layer continued as walls of the 21–27 nm wide tubules, which were traversing the episporontal space (Fig. 25, 26), and as the envelope of the sporophorous vesicle. The structure of the envelope changed from being uniform at the initiation (Fig. 10) to double-layered when surrounding mature spores (Fig. 22, 24). The tubules were probably filled with the same substance that made up the basal layer of the exospore, even if it was slightly less electron-dense. The walls of the tubules were not always apparent, and the traversing structures could erroneously be taken for fibrils. The great amount of tubules completely obscured the exospore (Fig. 21). The granular component of the episporontal space, which made sporogonial stages easily recognized in a stained preparation (Fig. 6–9, 14) disappeared when the material was organized into tubules, and mature spores lacked granulation completely (Fig. 15, 16).

As the spores were fairly large, the polar filament, even the coiled part, was clearly visible both in living and stained im-

mature spores (Fig. 16, 18). The filament was attached to a 670–680 nm wide, biconvex, stratified anchoring disc in the center of the apical end of the spore (Fig. 22, 23). It was posteriorly reinforced by a ring-like structure (Fig. 23). The straight, up to 330 nm wide, anterior part turned sideways approximately $\frac{1}{4}$ from the front end to touch the spore wall, and the final portion was arranged in 12–13, 191–264 nm wide, isofilar coils in one row close to the spore wall (Fig. 18, 22). The coils occupied approximately $\frac{1}{3}$ of the spore length, starting at the middle of the spore. The angle of tilt of the most anterior coil to the long axis of the spore was in most spores 85–90°, but angles down to 55° were measured. The last and most immature coil was often narrower. When squashed between a slide and coverglass some of the spores spontaneously ejected their polar filament. The longest ejected filament measured 235 μm . A drop-like body was normally visible at the apex of newly ejected filaments (Fig. 19).

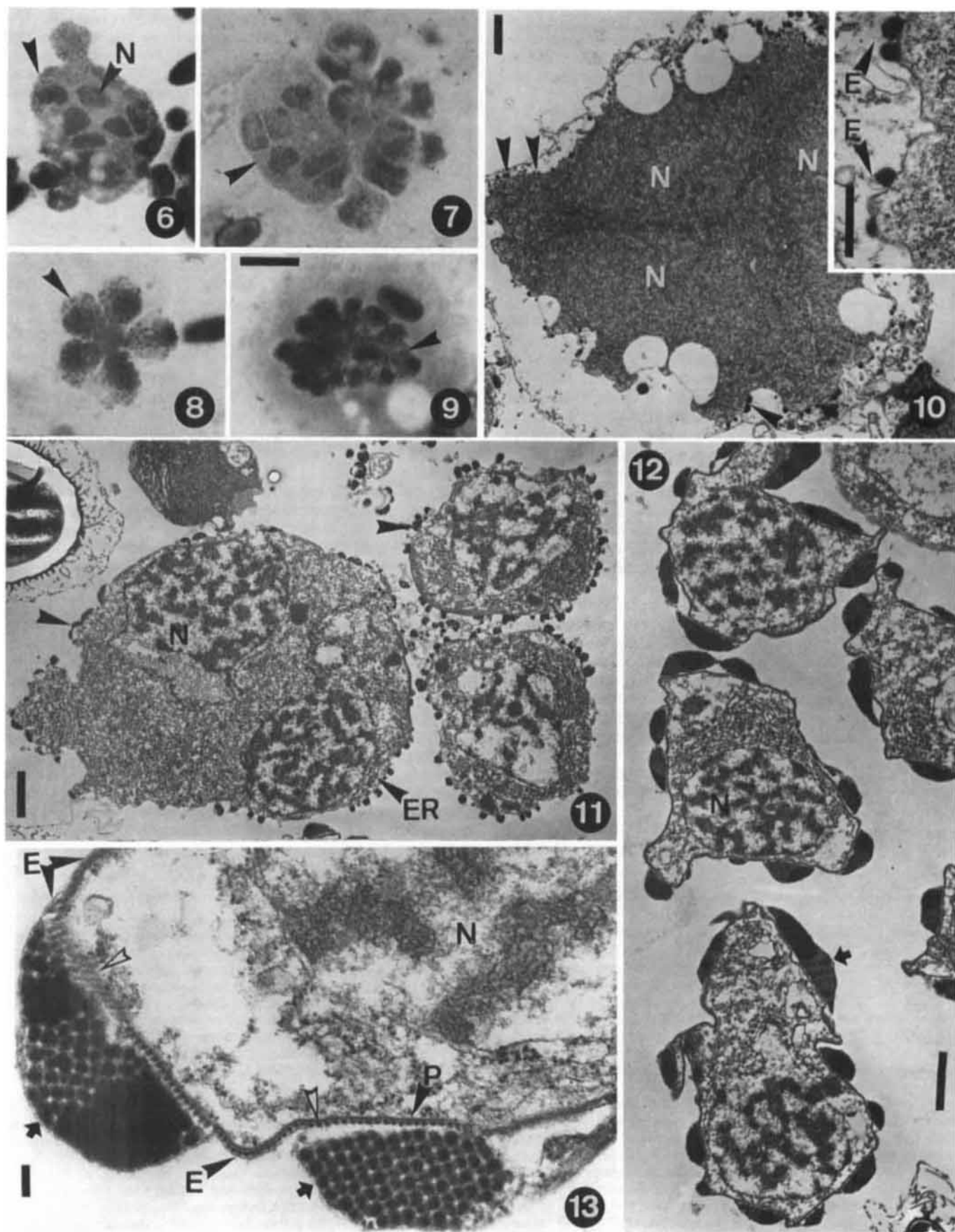
The transversely sectioned filament was stratified as follows (Fig. 28): 1) a granular center which was slightly less than half the diameter of the filament, 2) a fairly lucent layer measuring about half the filament radius, 3) an approximately 7 nm thick, moderately dense layer, and 4) an external unit membrane about 5 nm thick. The lucent part (2) had traces of concentrically arranged layers; the one closest to the periphery was the most distinct.

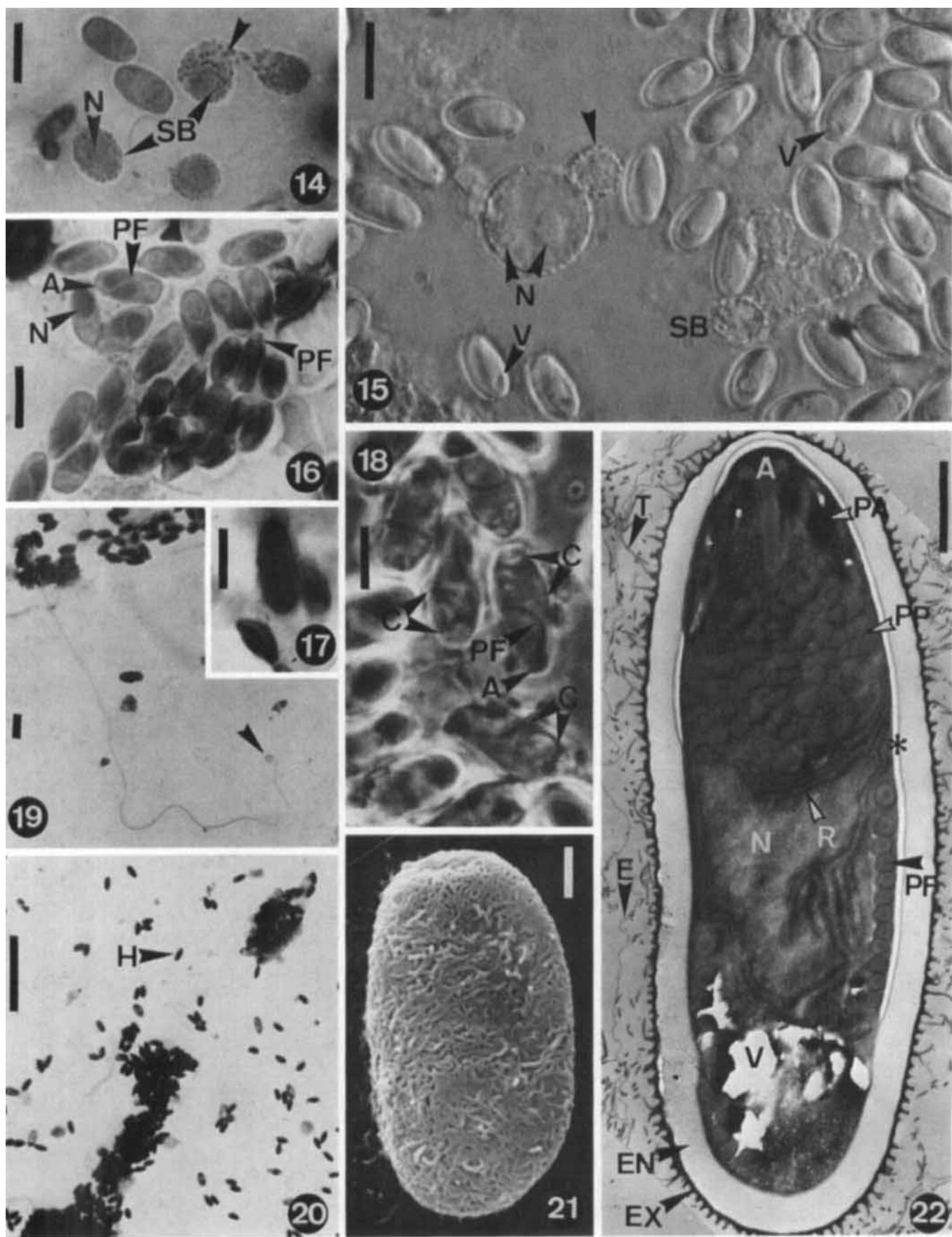
The polaroplast, surrounding the uncoiled part of the polar filament, tapered posteriorly towards the middle of the spore. It had two parts with chambers delimited by approximately 5-nm thick unit membranes. The lamellar chambers of the anterior part were so closely arranged that they lacked a lumen except at their periphery (Fig. 23). The lamellar polaroplast was bell-shaped, approximately 1.5 times as thick as the diameter of the polar filament, and extended backwards to the middle of the total polaroplast. The posterior portion of the polaroplast had up to 300-nm wide sac-like compartments, closely covering the polar filament (Fig. 22, 23, 27). The umbrella-like polar sac, which was filled with a moderately dense material, almost completely enclosed the lamellar polaroplast portion (Fig. 23).

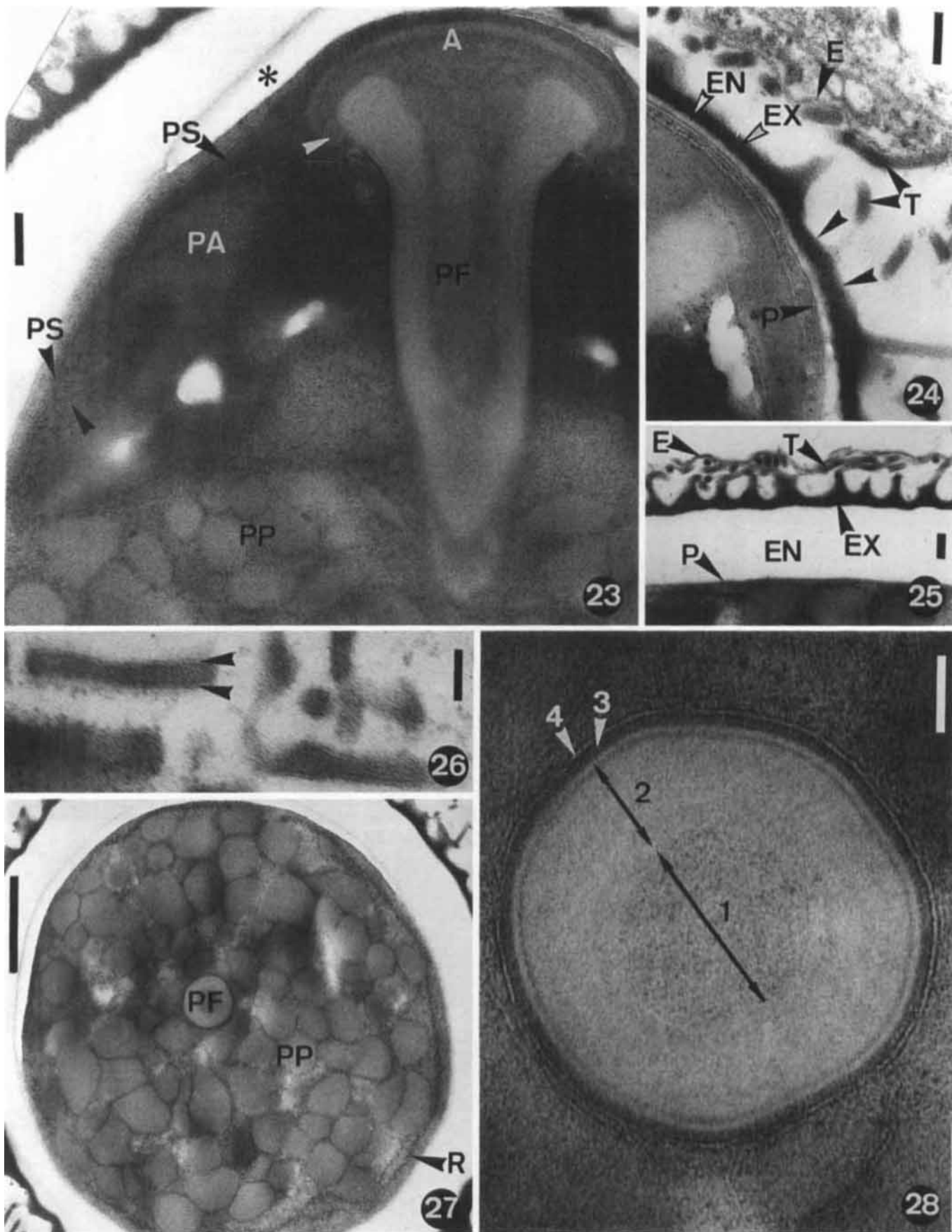
The irregularly shaped nucleus filled the center of the spore. The greatest sectioned nucleus measured 3.1 μm in diameter. The cytoplasm was granular and concentric layers of helically arranged, membrane-associated ribosomes (polyribosomes) surrounded the nucleus and the polaroplast (Fig. 22, 27). The posterior membrane-lined vacuole, measuring about $\frac{1}{6}$ of the spore length, was seen in an oblique position close to the end

Fig. 6–13. Sporogony. 6. Multinucleate sporogonial plasmodium; arrowheads indicate granules of the sporophorous vesicle (in Fig. 6–9). 7. Sporogonial plasmodium with lobes being formed. 8. Five-lobed sporogonial plasmodium. 9. Multilobed sporogonial plasmodium. 10. Sporogonial plasmodium with the first signs of the developing sporophorous vesicle (arrowheads). Inset: vesicle primordium at greater magnification. The cavity of the protuberances is more or less filled with electron-dense material. 11. Peripheral section of a lobed sporogonial plasmodium (the structures to the right, looking like free cells, are lobes). Protuberances (arrowheads) are more numerous and the dense inclusions are changing to more spongy structure. 12. Free sporoblasts enclosed in individual sporophorous vesicles. Protuberances are still prominent. Arrow, areas with visible paracrystalline structure. 13. Periphery of a sporoblast at greater magnification. Arrows, paracrystalline arrays; arrowheads, the fibrous primordia of the exospore. E, envelope of the sporophorous vesicle; ER, endoplasmic reticulum; N, nucleus and P, plasma membrane. Stains: 6, 8, 9, haematoxylin; 7, Giemsa. 10–13: ultrathin sections. Bars: 6–9 (with common bar on 9): 10 μm ; 10–12: 1 μm ; inset on 10: 0.5 μm ; 13: 100 nm.

Fig. 14–22. Spores. 14. Sporoblasts and immature spores. Arrowhead, granulation of the sporophorous vesicle. 15. Living sporogonial plasmodia, sporoblasts and mature spores. Arrowhead, vesicle granules. 16. Immature and mature spores (smaller and more intensely stained, to the right). The developing extrusion apparatus is visible in immature spores. 17. Macrospore. 18. Living immature spores; the polar filament, including the row of coils, is clearly visible. 19. Ejected polar filament; arrowhead, a blister-like body at the tip. 20. Slide No. 880719-H-7 RL, showing the localization of the holotype. 21. SEM-picture of a mature spore; tubules of the sporophorous vesicle are prominent. 22. Ultrathin longitudinal section of a mature spore showing the arrangement of the organelles and the individual sporophorous vesicle. * indicates an artifact. A, anchoring disc; C, coiled portion of the polar filament; E, envelope of the sporophorous vesicle; EN, endospore; EX, exospore; H, holotype; N, nucleus; PA, anterior portion of the polaroplast; PF, polar filament; PP, posterior portion of the polaroplast; R, ribosomes; SB, sporoblast; T, tubule and V, posterior vacuole. Stains: 14, 16, 17, 20, haematoxylin; 19, Giemsa. Bars: 14–17, 19, 10 μm ; 18, 5 μm ; 20, 50 μm ; 21–22, 1 μm .







of the spore (Fig. 15). The vacuole was poorly preserved in all spores prepared for electron microscopy (Fig. 22).

DISCUSSION

The family Tuzetiidae was established in 1977 to replace an unavailable name introduced in 1971 [12]. The family was characterized by a unique sporogony, where the sporophorous vesicle divided together with the sporogonial plasmodium, giving rise to sporoblasts enclosed in individual sporophorous vesicles. *Tuzetia* was the only genus. A contemporary study of *Plistophora debaisieuxi* Jírovec, 1943 revealed that the sporophorous vesicles divided in the way characteristic for *Tuzetia*, and the species was transferred to this genus [8]. By this action *Tuzetia* became heterogeneous in that *T. debaisieuxi* had nuclei in diplokaryotic arrangement in the early part of the life cycle, while the other species are entirely monokaryotic. Some years later two new genera, *Alfvenia* and *Janacekia*, were created to accommodate *Tuzetia*-like microsporidia which exhibit a life cycle with alternating diplo- and monokaryotic life cycle stages [6]. The new genera were included in Tuzetiidae, waiting for an analysis of the taxonomic potential of the nuclear configurations.

Alfvenia and *Janacekia* differ by the construction of the exospore and by the inclusions of the episporontal space [6]. *Alfvenia* has a plurilayered exospore and inclusions of the episporontal space are completely lacking, while *Janacekia* has a uniform exospore and tubular inclusions. The present microsporidium conforms with *Janacekia* in the life cycle, the shape of the spore and the ultrastructural cytology (the construction of the exospore, polaroplast, polar filament and the inclusions of the episporontal space). However, the inclusions of the episporontal space of the species described herein might give the impression of being fibrillar instead of tubular, as they were filled with a material of approximately the same density as the exospore (Fig. 26). The width of the tubules of the species under study equals the width of *Tuzezia* tubules, while the two previous *Janacekia* species have wider tubules. It is obvious that the width of the tubules of the episporontal space is not diagnostic for the genus. The two earlier species of *Janacekia* are parasites of blackfly larvae, and like the species treated herein, they use the adipose tissue for their development. The type species, *J. debaisieuxi*, exhibits a rare macrosporous sporogony together with the normal sporogony. The two blackfly parasites have distinctly smaller spores, where the length in fixed and stained condition does not exceed 5.3 μm . This difference in size clearly indicates that the species of blackflies and of *Ptychoptera* are distinct.

Few microsporidia have been reported from larvae of Ptychopteridae and Tipulidae. *Gurleya francottei* Léger and Duboscq, 1909, which is a parasite of *Ptychoptera contaminata* in France, is the only species found in Ptychopteridae. Tipulidae are hosts of three microsporidia: *Nosema stricta* Moniez, 1897, *Nosema binucleatum* Weissenberg, 1926, and *Thelohania tipulae* Weissenberg, 1926. *Gurleya francottei* and *N. binucleatum* are both parasites of the gut epithelium. The spores of the te-

trasporous *G. francottei* are 3 μm in length and pyriform [7]. Spores of *N. binucleatum* measure 2.6–2.85 \times 4.35–6.75 μm and are oval in shape [14]. *Thelohania tipulae* inhabits the adipose tissue, producing octosporous, oval, 3 \times 5 μm spores [14]. *Nosema stricta* is actually a *nomen nudum* [12]; the size of the spores, 1.5 \times 5 μm , is all that is known about the species [9]. Even if it unclear if these spore sizes refer to living or stained spores, all four microsporidian species described from larvae of Ptychopteridae and Tipulidae have distinctly smaller spores than the species treated herein.

There is nothing remarkable about the cytology and life cycle of the microsporidium described herein; however, the fact that the exospore is initiated as closely arranged fibrous material (Fig. 11) is new to the Tuzetiidae. This resembles the initiation observed in some microsporidia devoid of sporophorous vesicles, for example *Encephalitozoon cuniculi* [1], *Nosema tractabile* [5] and *Unikaryon slaptoneleyi* [3], where the exospore primordia appear as equidistant parallel strands of electron-dense material. The regularly arranged structures seen in the sporogony of *Berwaldia singularis* might look similar, but these are tubules, not fibrils, and they constitute the internal layer of a two-layered sporophorous vesicle [4].

Description

Janacekia adipophila n. sp.

Merogony. Diplokaryotic, producing at least five merozoites per meront. The number of merogonic cycles is unknown.

Sporogony. A diplokaryotic sporont yields a multinucleate plasmodium with isolated nuclei, which divides into 8–16 uniciliate sporoblasts by rosette-like division. The first division of the sporont is probably reductional.

Spores. Unfixed spores measure 4.2–6.3 \times 9.1–11.2 μm , fixed and stained spores 3.8–5.6 \times 7.1–9.6 μm . A rare macrosporous sporogony produces large spores up to 6.7 \times 16.5 μm (fixed and stained). The spore wall is 106–490 nm thick with a 34–170 nm thick exospore ornamented with ridges. The exospore is electron-dense with a double-layer covering. The polar filament has 12–13, 191–264 nm wide, isofilar coils in a single layer close to the spore wall in the posterior half of the spore. The row of coils is approximately $\frac{1}{3}$ of the spore length. The angle of tilt is 85–90° (exceptionally down to 55°). The regularly arranged anterior polaroplast lamellae are tightly compressed. The posterior sac-like polaroplast compartments are up to 300 nm wide. The polaroplast ends close to the anterior filament coil in the middle of the spore. A single nucleus is found in the center of the spore.

Sporophorous vesicle. Initiated by the sporogonial plasmodium and dividing together with the plasmodium to produce sporoblasts in individual vesicles. Sporogonial plasmodia and sporoblasts appear prominently granular under the light microscope due to the accumulation of material in the episporontal space. Immature and mature spores have 21–27 nm wide tubules connecting the envelope of the vesicle with the exospore.



Fig. 23–28. Ultrastructure of the spore. 23. Anterior end of a mature spore exhibiting the anchoring apparatus, the anterior part of the polar filament and the two parts of the polaroplast. White arrowhead, the ring-like structure at the posterior edge of the anchoring disc. Black arrowhead, the wider peripheral parts of the anterior polaroplast lamellae. * indicates an artifact. 24. The three-layered spore wall at the anterior pole and a part of the sporophorous vesicle. Arrowheads, the double-membrane like surface layer of the exospore. 25. The exospore exhibits a system of regularly arranged ridges. Tubules connect the exospore with the envelope of the sporophorous vesicle. 26. Longitudinally sectioned tubules of the sporophorous vesicle. The walls have double-membrane construction (arrowheads). 27. Transversely sectioned polar filament; numbers indicate the principal layers. A, anchoring disc; E, envelope of the sporophorous vesicle; EN, endospore; EX, exospore; P, plasma membrane; PA, anterior part of the polaroplast; PF, polar filament; PP, posterior part of the polaroplast; PS, polar sac; R, ribosomes and T, tubules. Bars: 23–25, 100 nm; 26, 28, 50 nm; 27, 0.5 μm .

Host tissues involved. Fat cells, which are disintegrated to a syncytium. Nuclei of host cells are hypertrophic.

Type host. Larvae of *Ptychoptera paludosa* Meigen, 1804 (Diptera, Ptychopteridae).

Type locality. The small river Vege å, at Knutstorp, Scania, in the south of Sweden.

Types. Holotype (Fig. 20) on slide No. 880719-H-7 RL, paratypes on slides No. 880719-H-(1-8) RL.

Deposition of types. The slide with the holotype in the International Protozoan Type Slide Collection at Smithsonian Institution (Washington, DC). Paratypes in the collections of Dr. J. Weiser, Prague (Czechoslovakia) and in the collection of the author.

Etymology. Alluding to the tissue affinity.

ACKNOWLEDGMENTS

The author is indebted to Mrs. Lina Hansén, Mrs. Inga Jogby, Mrs. Birgitta Klefbohm, Mrs. Inger Norling and Mrs. Inga-Lill Palmquist, all at the Department of Zoology, University of Lund, for excellent technical assistance, and to Dr. Hugo Andersson for the identification key to *Ptychoptera* larvae. The investigation was supported by research grants from the Swedish Natural Science Research Council.

LITERATURE CITED

1. Barker, R. J. 1975. Ultrastructural observations on *Encephalitozoon cuniculi* Levaditi, Nicolau et Schoen, 1922, from mouse peritoneal macrophages. *Fol. Parasitol., Praha*, **22**:1-9.
2. Brindle, A. 1962. Taxonomic notes on the larvae of British Diptera 9. The family Ptychopteridae. *The Entomologist*, **94**:212-216.
3. Canning, E. U., Barker, R. J., Hammond, J. C. & Nicholas, J. P. 1983. *Unikaryon slptonleyi* sp. nov. (Microspora: Unikaryonidae) isolated from echinostome and strigeid larvae from *Lymnaea peregrina*: observations on its morphology, transmission and pathogenicity. *Parasitology*, **87**:175-184.
4. Larsson, R. 1981. A new microsporidium *Berwaldia singularis* gen. et sp. nov. from *Daphnia pulex* and a survey of microsporidia described from Cladocera. *Parasitology*, **83**:325-342.
5. Larsson, R. 1981. Description of *Nosema tractabile* n. sp. (Microspora, Nosematidae), a parasite of the leech *Helobdella stagnalis* (L.) (Hirudinea, Glossiphoniidae). *Protistologica*, **17**:407-422.
6. Larsson, R. 1983 (published 1984). A revisionary study of the taxon *Tuzetia* Maurand, Fize, Fenwick and Michel, 1971, and related forms (Microspora, Tuzetiidae). *Protistologica*, **19**:323-355.
7. Léger, L. & Duboscq, O. 1909. Protistes parasites de l'intestin d'une larve de *Ptychoptera* et leur action sur l'hôte. *Bull. Acad. R. Belg., Cl. Sci.*, **8**:885-902.
8. Loubès, C. & Maurand, J. 1976. Étude ultrastructurale de *Pleistophora debaisieuxi* Jirovec, 1943 (Microsporida); son transfert dans le genre *Tuzetia* Maurand, Fize, Michel et Fenwick, 1971 et remarques sur la structure et la genèse du filament polaire. *Protistologica*, **12**:577-591.
9. Moniez, R. 1887. Observations pour la révision des Microsporides. *C. R. Acad. Sci., Paris*, **104**:1312-1314.
10. Reynolds, E. S. 1963. The use of lead citrate at high pH as an electron-opaque stain in electron microscopy. *J. Cell Biol.*, **17**:208-212.
11. Romeis, B. 1968. Mikroskopische Technik. Oldenbourg Verlag, München & Wien.
12. Sprague, V. 1977. Annotated list of species of microsporidia. In: Bulla Jr., L. A. & Cheng, T. C. (ed.), Comparative Pathobiology, Vol. 2. Plenum Press, New York, pp. 31-334.
13. Tjeder, B. 1968. Notes on the Scandinavian Ptychopteridae, with description of a new species (Diptera). *Opusc. Ent.*, **33**:73-79.
14. Weissenberg, R. 1926. Mikrosporidien aus Tipuliden-Larven. *Arch. Protistenkd.*, **54**:431-467.

Received 10-9-91, 1-28-92; accepted 2-4-92